

Thermo physical and Flow Properties of CO₂ Hydrate Slurry

Osmann SARI^{1*}, Jin HU¹, Sara EICHER¹, Peter W. EGOLF¹, Paul HOMSY²

¹ Institute of Thermal Engineering, University of Applied Sciences of Western Switzerland
Avenue des Sports 14, 1400 Yverdon-les-Bains, Vaud, Switzerland
Contact Information (+41 (0) 79 647 21 30, Osmann.sari@heig-vd.ch)

² Nestec,
Avenue Nestlé 55,
1800 Vevey, Switzerland

ABSTRACT

The apparent viscosity and flow regime of CO₂ hydrate slurry were investigated with a XL7-100 on-line resonant viscometer. Possible reasons for the viscosity changes before and after the nucleation of hydrates are discussed. In addition, super saturation of the CO₂ solution under certain pressure and temperature conditions as well as its density and apparent viscosity were examined. The hydrate's solid fraction and the dissociation enthalpy were evaluated by an on-line Micro DSC system. Real-time coupled multi-electrode array sensor (CMAS) probes were applied to measure the maximal localized corrosion rate of three different materials subjected to CO₂ hydrate slurry and saturated CO₂ solution in the temperature range of 1 to 18 °C and pressure range of 25 to 30 bar. The density of CO₂ hydrate slurry was also experimentally investigated and the relation between the density and the solid fraction has been established.

1. INTRODUCTION

The synthetic refrigerants impact on the environment and newly imposed safety measures force the cooling industry to seek for solutions to remove certain gases or to decrease their content in numerous different systems. During the last ten years the load reduction of refrigerants in installations and the development and use of natural, non-flammable and environment preserving cooling agents became the two preferred methods to improve the current situation. The creation of hydrates – a kind of multifunctional thermal fluid – is one of these promising technologies.

CO₂ hydrates are obtained by the combination of water and CO₂ (gas) under defined conditions of temperature and pressure. CO₂ hydrate slurry is one of the promising recently proposed secondary refrigerants in order to phase out CFC's and HCFC's. CO₂ hydrate slurry is suitable for cooling applications, because its melting point is adjustable by changing the production conditions and can be even applied to the positive temperature range (+5 to +7 °C), which are temperatures required in air-conditioning systems. Pure CO₂ hydrate has a dissociation enthalpy of 500 kJ/kg of water, being 1.5 times higher than that related to the ice crystal melting. It also displays an excellent ability to be pumped. In order to use CO₂ hydrate slurry efficiently, not only the intrinsic thermal properties must be known but also rheological data is required.

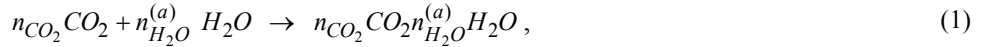
CO₂ hydrate slurry is produced by high pressure CO₂ gas injection in a cooled water solution. This work investigates CO₂ hydrate slurry produced with harmless CO₂, an inoffensive gas (potential of the ozone depletion layer: ODP = 0 and greenhouse effect: GWP (100a) = 1) in order to produce and to use CO₂ hydrate slurry continuously. Note that here CO₂ is recovered from existing industrial processes, for example fermentation, and is not specially produced for the purpose. The process could contribute to replace polluting fluids that will be prohibited from the beginning of the year 2010 on in the EU countries. Consequently, a high potential market is arising.

The objective of this paper is to present recent results and new findings regarding density, apparent viscosity, dissociation enthalpy, corrosion rate of CO₂ hydrate slurry in order to prove that CO₂ hydrate slurry as an environmental friendly refrigerant has thermal physical characteristics that are well-suited for refrigeration applications, especially in the field of air conditioning.

2. CO₂ HYDRATE AND CO₂ HYDRATE SLURRY PROPERTIES

2.1 Conservation Equations

Hydrates are non-stoichiometric crystalline compounds formed by cavities of “host” water molecules. Under certain pressure and temperature conditions they are strongly hydrogen bonded with a small guest molecule hydrate structure. There are two types of CO₂ hydrate, namely hydrate I with structure I and hydrate II with structure II respectively. CO₂ molecules can easily occupy 75% of the cavities of the structure I, but only 33% of the cavities of structure II. Structure type I hydrates consist of two small cages and six large cages. S I hydrate has the pentagonal dodecahedron (5¹²) as the small cage, the tetrakaidecahedron (5¹²6²) as the large cage. Therefore, in practice, hydrate I is the most common structure occurring in CO₂ hydrates. Hereafter, only hydrate I will be referred to as CO₂ hydrate. The chemical reaction equation for the hydration is:



where n_{CO_2} is the number of moles of CO₂ and $n_{H_2O}^{(a)}$ denotes the number of moles participating actively in the hydration process. Later we introduce $n_{H_2O}^{(i)}$, which is the number of moles not participating in hydration, characterizing the inactive water molecules. This equation is divided by n_{CO_2} to obtain:



where

$$n = \frac{n_{H_2O}^{(a)}}{n_{CO_2}} \quad (3)$$

is the ratio of the mole number of active water molecules divided by the mole number of present CO₂ molecules. The number n is also named the hydration number. It varies with pressure and temperature. One notifies that for our considerations:

$$5 < n < 7. \quad (4)$$

Then, for the total number of water moles, it follows that:

$$n_{H_2O} = n_{H_2O}^{(a)} + n_{H_2O}^{(i)}. \quad (5)$$

The mole numbers could be split further to the atomic level, which is not necessary here. Analogous the active part of the water can be distinguished from the inactive. A basic equation is:

$$m_\alpha = n_\alpha M_\alpha, \quad \alpha \in \{ CO_2, H_2O, \dots \}. \quad (6a, b, \dots)$$

By multiplying Eq. (5) with M_{H_2O} and applying Eq. (6) one obtains:

$$m_{H_2O} = m_{H_2O}^{(a)} + m_{H_2O}^{(i)}. \quad (7)$$

The mass of CO₂ - according to Eq. (6) - is:

$$m_{CO_2} = n_{CO_2} M_{CO_2}. \quad (8)$$

The mass of the hydrate is:

$$m_{Hydrate} = m_{CO_2} + m_{H_2O}^{(a)}, \quad (9)$$

respectively with Eq. (6):

$$m_{Hydrate} = n_{CO_2} M_{CO_2} + n_{H_2O}^{(a)} M_{H_2O}. \quad (10)$$

The mass of the fluid is:

$$m_{Fluid} = m_{CO_2} + m_{H_2O} = m_{CO_2} + m_{H_2O}^{(a)} + m_{H_2O}^{(i)} = m_{Hydrate} + m_{H_2O}^{(i)}, \quad (11a-c)$$

where Eq. (7) and (9) were substituted into (11a,b) to obtain (11b,c). With Eq. (6) it follows that:

$$m_{Fluid} = n_{CO_2} M_{CO_2} + n_{H_2O} M_{H_2O} = n_{CO_2} M_{CO_2} + (n_{H_2O}^{(a)} + n_{H_2O}^{(i)}) M_{H_2O}. \quad (12a, b)$$

$$M_C = 12.011 \text{ kg/kmole} \quad M_O = 15.999 \text{ kg/kmole} \quad M_{CO_2} = 44.009 \text{ kg/kmole} \quad (13a-c)$$

$$M_H = 1.008 \text{ kg/kmole} \quad M_{H_2O} = 18.015 \text{ kg/kmole} \quad (14a,b)$$

In a practical application we know the total mass of CO_2 and H_2O . Then the small theory gives the mass of hydrate present in the fluid. For this we apply Eq. (3) and (10) to obtain:

$$m_{\text{Hydrate}} = \left(M_{CO_2} + \frac{n_{H_2O}^{(a)}}{n_{CO_2}} M_{H_2O} \right) n_{CO_2} = (M_{CO_2} + n M_{H_2O}) n_{CO_2}. \quad (15a,b)$$

$$m_{\text{Hydrate}} \approx (44 + 18 n) n_{CO_2} \approx 152 n_{CO_2}. \quad (16)$$

One can also write:

$$m_{\text{Hydrate}} = (M_{CO_2} + n M_{H_2O}) \frac{m_{CO_2}}{M_{CO_2}} = \left(1 + n \frac{M_{H_2O}}{M_{CO_2}} \right) m_{CO_2}. \quad (17a,b)$$

With the concrete values it follows that:

$$m_{\text{Hydrate}} \approx 3.68 m_{CO_2}, \quad \text{if } n = 6. \quad (18)$$

2.2 Density Models

Determination of the density of either water or carbon dioxide is based on an equation of state (EoS) in the form of a fundamental equation explicit in the Helmholtz free energy, which is solved from known temperature and pressure conditions. The region of interest lies between $273.15 < T < 293.15$ K and $1 < p < 40$ bar.

Helmholtz function

The fundamental equation of state (EoS) to describe the properties of both, ordinary water and the carbon dioxide, is expressed in form of the Helmholtz energy:

$$\phi(\delta, \tau) = \phi^{(0)}(\delta, \tau) + \phi^{(\tau)}(\delta, \tau) \quad (19)$$

where $\delta = \rho/\rho_c$ is the reduced density and $\tau = T_c/T$ is the inverse reduced temperature. Both, the density ρ and the temperature T are reduced with their critical values ρ_c and T_c , respectively.

The critical values for ordinary water and carbon dioxide are given in Table 1.

Table 1: Critical value for ordinary water and carbon dioxide.

Critical Point	Ordinary Water	Carbon Dioxide
Temperature, K	647.096	304.128
Pressure, bar	220.64	73.77
Density, kg/m ³	322.0	467.6

Density of water

The density of ordinary water was calculated from the IAPWS-95 EoS derived by Wagner and Pruss (2002). This formulation covers both, the gas and liquid regions for the state of water; our interest remains focussed on the liquid region. The estimated uncertainty is reported to have a maximal error in the density of 0.02 %.

Density of carbon dioxide

The density of CO_2 was defined with the EoS formulation developed by Span and Wagner (1996). This formulation covers both gas and liquid regions, but our interest is focused on the gas domain. The estimated relative uncertainty of the density is reported to have a maximal value of 0.05 %.

Density of CO_2 solution

The density model proposed by Duan *et al.* (2008) for liquid CO_2 - H_2O mixtures, hereafter referred as CO_2 solution, was defined using the equation:

$$\rho_{CO_2HO} = \frac{M_{CO_2-H_2O}}{V_{CO_2-H_2O}} \quad (20)$$

$$M_{CO_2-H_2O} = x_{CO_2} M_{CO_2} + x_{H_2O} M_{H_2O} \quad (21)$$

$$V_{CO_2-H_2O} = V_1 [1 + (A_1 + A_2 P)x_{CO_2}] \quad (22)$$

$$A_i = A_{i1}T^2 + A_{i2}T + A_{i3} + A_{i4}T^{-1} + A_{i5}T^{-2} (i=1,2) \quad (23a,b)$$

$\rho_{CO_2-H_2O}$ is the density of the CO_2 solution, $V_{CO_2-H_2O}$ is the molar volume of the CO_2 solution, P is the pressure (in MPa), T the temperature (in K) and M and x are the molar mass and the mole fraction, respectively. The mole fractions are calculated as:

$$x_{CO_2} = \frac{\frac{m_{CO_2}}{M_{CO_2}}}{\frac{m_{CO_2}}{M_{CO_2}} + \frac{1}{M_{H_2O}}} \quad (22a)$$

and

$$x_{H_2O} = 1 - x_{CO_2} \quad (22b)$$

where m_{CO_2} is the CO_2 solubility in water (in g/g) proposed by Duan *et al.* (2006) and M is as the same as in Eq. 21.

Density of CO_2 pure hydrate

Teng *et al.* (1996) indicated that CO_2 hydrate is a well-defined crystalline compound, the density of CO_2 hydrate ρ_H can be predicted accurately based on the unit cell as:

$$\rho_{hydrate} = \frac{46 \cdot M_{CO_2}}{N_0 \cdot a^3} \left(0.409 + \frac{x_{CO_2}^{hydrate}}{1 - x_{CO_2}^{hydrate}} \right) \quad (23)$$

where 46 is the number of water molecules in a unit CO_2 hydrate cell, M_{CO_2} is the mole mass of CO_2 in g/mol, $M_{CO_2} = 44$ g/mol, N_0 is the Avogadro constant 6.0225×10^{23} /mol, a is the lattice parameter of a unit cell of Structure I hydrate. $a = 11.956 \text{ \AA} \approx 12 \text{ \AA} = 12 \times 10^{-10} \text{ m}$ $a^3 = (12 \times 10^{10})^3 \text{ m}^3 = 1.728 \times 10^{-27} \text{ m}^3$. The mole fraction of CO_2 in the CO_2 hydrate, denoted as $x_{CO_2}^{hydrate}$. As the chemical formula for CO_2 hydrate is $(x + y) CO_2 \cdot 46H_2O$, so $x_{CO_2}^{hydrate}$ can be expressed as:

$$x_{CO_2}^{hydrate} = \frac{CO_2}{CO_2 + \frac{46}{x+y} H_2O} \quad (24)$$

Here x (≤ 2) and y (≤ 6) represent the numbers of the occupied small and large cavities, respectively. $x+y \leq 8$, 46 is the number of water molecules in a unit CO_2 hydrate cell.

Density of CO_2 hydrate slurry

The density of hydrate slurry can be derived from a mass balance where the mass of free CO_2 gas in the hydrate slurry can be neglected due to the very small amount and not considered in the equation:

$$\rho_{hydrate, slurry} = \frac{\rho_{liquid} \cdot \rho_{hydrate}}{\rho_{liquid} \cdot x_{hydrate} + \rho_{hydrate} (1 - x_{hydrate})} \text{ and } x_{liquid} + x_{hydrate} = 1 \quad (25a,b)$$

where ρ is the density, m is the mass, x_{liquid} is the liquid mass fraction in the hydrate slurry and $x_{hydrate}$ is the hydrate concentration (solid fraction) in the hydrate slurry.

2.3 Dynamic Viscosity Models

Viscosity of water

The equation presented by Watson *et al.* (1980) for the dynamic viscosity of water substance was adopted in this work:

$$\eta_{H_2O} = \eta_0(T) \exp \left[\rho^* \left\{ \sum_{i=0} \sum_{j=0} a_{ij} (T^{*-1} - 1)^i (\rho^* - 1)^j \right\} \right] \quad (26)$$

where

$$\frac{\eta_0(T)}{10^{-6} \text{ Pas}} = \sqrt{T^*} \left[\sum_{k=0}^3 \left(\frac{a_k}{T^{*k}} \right) \right]^{-1} \quad (27)$$

The reduced temperature, T^* , and reduced density, ρ^* , are defined relative to the critical values, (see Table 1):

$$T^* = T/T_c \text{ and } \rho^* = \rho/\rho_c \quad (28)$$

The coefficients a_{ij} and a_k can be found in Watson *et al.* (1980).

Viscosity of carbon dioxide

The viscosity of carbon dioxide was modelled with an equation taken from the work of Fenghour *et al.* (1998):

$$\eta_{CO_2} = \eta_0(T) + \sum_{i=1}^n \left(\sum_{j=1}^m d_{ij} / T^{*(j-1)} \right) \rho^i \quad (29)$$

and

$$\eta_0(T) = \frac{1.00697 T^{1/2}}{\exp \left(\sum_{i=0}^4 a_i (\ln T^*)^i \right)} \quad (30)$$

with coefficients a_i and d_{ij} provided in Fenghour *et al.* (1998). The reduced temperature, T^* , is given by:

$$T^* = kT/\varepsilon \text{ and } \varepsilon/k = 251.196 \text{ K}$$

Viscosity of CO₂ solution

The viscosity of the CO₂ solution was reproduced using the simple empirical equation proposed by Grunberg and Nissan (1949):

$$\eta_{CO_2-H_2O} = \exp(x_{CO_2} \ln \eta_{CO_2} + x_{H_2O} \ln \eta_{H_2O} + x_{CO_2} (1 - x_{CO_2})^* G) \quad (31)$$

with x_{CO_2} and x_{H_2O} calculated with Eq. (22) and η_{H_2O} and η_{CO_2} with Eq's. (26) and (29), respectively. G is the only adjustable parameter that can be calculated from experimental results.

Viscosity of CO₂ hydrate slurry

Up to now, not so much information is available regarding the viscosity of CO₂ hydrate slurry. Only few authors have experimentally investigated the viscosity of CO₂ hydrate slurry. H.Oyama *et al.* (2003) argue that the large number of water molecules tends to construct precursor hydrogen-bonded structures in the solution leading to an increase in the viscosity prior to the hydrate formation. Andersson (1999) and Andersson and Dudmundsson (2000) have also reported that the slurry viscosity increases with increasing hydrate concentration.

2.4 Enthalpy of Hydrate Fusion

The formation of gas hydrate is an exothermic equilibrium process. The dissociation of gas hydrate is an endothermic equilibrium process. To use this endothermic process is to benefit from the latent heat of fusion of the CO₂ hydrate phase change. As an example, Bozzo *et al.* (1975) have reported an enthalpy of dissociation of 58.16 kJ/mol at 10 °C and for the carbon dioxide hydrates a hydration number of 7.03.

3. EXPERIMENTAL TEST FACILITY

An experimental loop was built up to study production, storage, transport and use of CO₂ hydrate slurry as newly developed refrigerant. In addition it is used to characterise the thermal-physical properties of the CO₂ hydrate slurry. A new temperature sensor was developed in collaboration with Roth + CO AG. The objective was to obtain a high precision temperature measurement in a point. The sensor diameter is 2 mm and the sensitive layer is 1.6 mm high by 1.2 mm long. The mass flow rate of all working fluids in the experimental rig was measured by Endress+Hauser mass flow meters. Densities of water, CO₂ solution as well as CO₂ hydrate slurry are measured by mass flow meters of Endress+Hauser, which were calibrated according to the suitable temperature and pressure range for hydrate formation and dissociation. The heat capacity and enthalpy are measured by a digital scanning calorimetry (DSC). There is a new innovative device XL7-100 viscometer to measure on-line the fluid viscosity. The XL7-100 viscometer produced by Hydramotion Ltd. in UK is a class of instruments called vibrational or resonant viscometers. Real-time coupled multi electrode array sensor (CMAS) probes were used to measure the maximal localised corrosion rate of type 1018 low carbon steel, copper 110 and 304L stainless steel in CO₂ hydrate slurry and saturated CO₂ solution in the temperature range 1 to 18 °C and pressure range 25 to 30 bar.

4. RESULTS AND DISCUSSION

4.1 Density and Viscosity Results

Density and viscosity of water

The density and viscosity of tap water under atmosphere and dynamic conditions was measured online by a mass flow meter at temperatures between 1 and 29 °C. The temperature of the water in the loop was first set at 29 °C and then cooled down continuously to 1 °C. The velocity of water in the loop was about 1 m/s driven by a high pressure pump. This experiment was repeated three times under the same experimental conditions to evaluate the measurement deviations. The maximal deviation between the density measurements was estimated to be 2.2 %. As expected, the density decreases with increasing temperature. Results obtained from water EoS proposed by Wagner and Pruess (2002) were used for comparison purposes. The experimental values are in a good agreement with the literature data with a maximal deviation of 5.5 % found at lower temperatures. Measurement of the viscosity of tap water under atmospheric conditions was performed to evaluate the “resonance” method of the XL7-100 viscometer, employed to record online the fluid viscosity. The maximal deviation between measurements was estimated to be 3.5 %. The experimental values are in good agreement with the viscosity equation proposed by Watson *et al* (1980) and the absolute deviation is within 4 %. The “resonance” method, which is proposed in this study, can be applied to determine the viscosity of the fluid with a maximal uncertainty of 4.5 %.

Density and viscosity of the CO₂ solution

CO₂ solution density and viscosity measurements were also undertaken at four different temperatures: 7, 8, 9 and 10 °C. Figure 1a shows the temperature and pressure dependence of the density of the CO₂ solution. It can be seen that density decreases with increasing temperature, but increases with increasing pressure. It follows the behaviour reported by other investigators such as Garcia (2000), who also indicated that CO₂ saturated water was heavier than ordinary water. In a similar manner to the density description, the viscosity of the CO₂ solution was also found to decrease with increasing temperature and to increase with increasing pressure. This indicates that high pressures and low temperatures aid more CO₂ gas to be dissolved into water, resulting in a higher viscosity of the solution. In other words, the viscosity of the CO₂ solution depends on the CO₂ solubility.

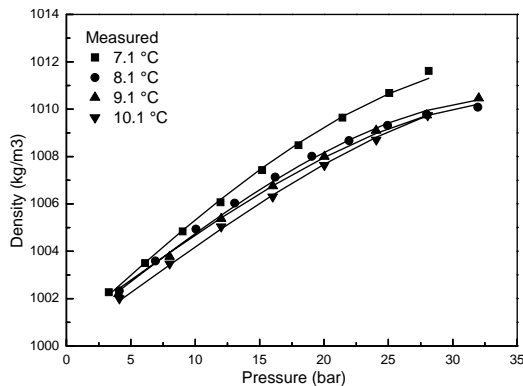


Figure 1a: Density of the CO₂ solution as function of pressure and temperature.

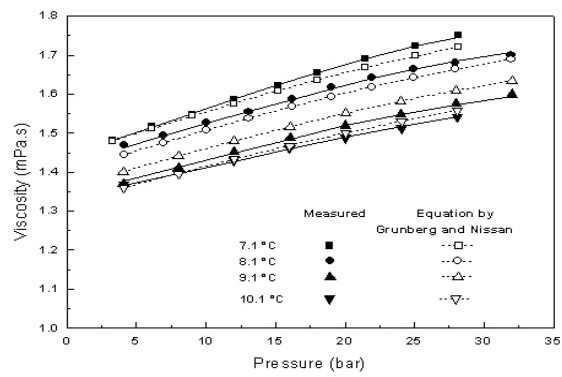


Figure 1b: The pressure and temperature dependence of the CO₂ solution viscosity.

Experimental results were also compared with Grunberg and Nissan's (1949) correlation for viscosity of liquid mixtures. The only adjustable parameter in this equation, G , was calculated using the experimental data and literature values for viscosity of CO₂ gas and water. The parameter G was found to be dependent on the CO₂ mole fraction and was therefore described using a polynomial function.

Viscosity of CO₂ solution and CO₂ hydrate slurry at different density values

The tap water in the experimental loop was cooled down simultaneously by two chillers to 1.5 °C. The velocity of the water was about 1 m/s. Afterwards, CO₂ gas was injected into the water several times to form a CO₂ solution and, thereafter, a CO₂ hydrate slurry (see in Figure 2, which shows the general appearance of the CO₂ hydrate slurry). The temperature setting for the two chillers was kept at 1 °C during the whole experiment. The safety pressure regulation for the loop is 37 bar. After each injection, fluid in the loop was left to stabilize for several minutes. The temperature, pressure, viscosity and density of water, saturated CO₂ solution as well as CO₂ hydrate slurry were measured, the

average values of the above variables under stable conditions were derived, see Figure 3, where each scan corresponds to 5 seconds.



Figure 2: Appearance of CO_2 hydrate slurry.

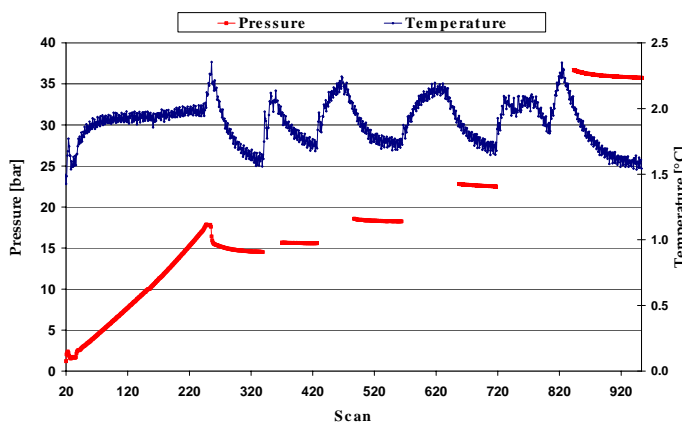


Figure 3a: Temperature and pressure profile in the loop during the experiment

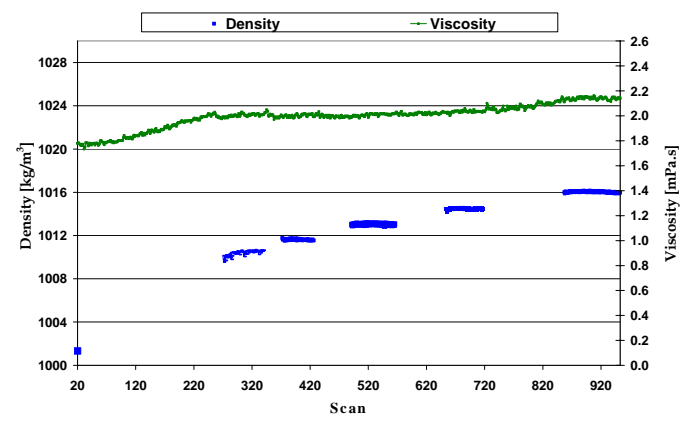


Figure 3b: Viscosity as function of solution density during the experiment

From Figure 3 it can be seen that during the entire experiment, the fluid underwent three different states, namely liquid water, CO_2 solution, and CO_2 hydrate slurry, respectively. However, the temperature of the fluid was not much influenced by the phase transition and was regulated by the two chillers whose fluctuations varied between 1.5 to 2.3 °C.

Table 2: Properties for water, CO_2 solution and CO_2 hydrate slurry at different loop conditions.

Fluid	Average Pressure (bar)	Temperature range (°C)	Average Density (kg/m^3)	Average Viscosity (mPa.s)
Water	1	1.5	1001.2	1.78
CO_2 solution	1-17.6 (unstable)	1.5-2	1001.2-1010 (unstable)	1.78-2
CO_2 hydrate slurry	14.7	1.6 - 2.2	1010	2
CO_2 hydrate slurry	15.6	1.7-2.0	1011.6	2
CO_2 hydrate slurry	18.3	1.7-2.0	1013	2.01
CO_2 hydrate slurry	22.6	1.75-2.0	1014.5	2.01-2.05
CO_2 hydrate slurry	36	1.6-1.95	1016	2.14

Initially the water in the loop was at 1 bar and 1.5 °C for which a viscosity of 1.78 mPa.s and a density of 1001.2 kg/m^3 were recorded. During several injections of CO_2 gas into the closed circuit, the pressure in the loop was gradually increased. This was followed by an increase in the viscosity and density of the fluid. Hydrate formation was only detected after scan 258 when the CO_2 solution changed into CO_2 hydrate slurry. A pressure drop of about 2.5 bar was observed during the formation of hydrates. The properties of water, CO_2 solution and CO_2 hydrate slurry are compared at different loop conditions in Table 2.

This experiment shows that within the temperature range of 1.5 to 2 °C, as pressure increases, so does the average density and viscosity of the fluid. However, after formation of CO₂ hydrates in the solution, despite the large increase of pressure in the loop (14.7 to 36 bar), the density of the fluid varied from 1010 to 1016 kg/m³, while the viscosity of the fluid only increased 7 %. This implies that CO₂ hydrate solid particles may contribute only slightly to the viscosity increase. In contrast, when the initial water transformed into the CO₂ solution prior to CO₂ hydrate formation within the same temperature range of 1.5 to 2 °C, pressure was increased from 1 to 17.6 bar, the density from 1001.2 to 1010 kg/m³, while the increase of viscosity was about 12 %. This suggests that the number of dissolved CO₂ molecules increases with the increase of pressure as well as the interaction between the CO₂ molecules and the water molecules, which will result in a viscosity increase. In addition, in this temperature range, when the CO₂ gas pressure is high (over 15 bar) a large number of hydrogen-bonded CO₂ hydrate precursor may form in the solution before nucleation of hydrates that also cause the increase of viscosity. These results provide evidence to the arguments advanced by Uchida *et al.* (2003) and Oyama *et al.* (2003).

4.2 Dissociation Enthalpy of CO₂ Hydrate

Preliminary measurements of specific heat of tap water were performed with the Micro DSC VII to test the accuracy and reliability of the procedure before applying it to measure dissociation enthalpy of CO₂ hydrate. Within narrow limits, the same pattern is obtained in both curves. Reported values of specific heat of water varied from 4.178 to 4.211 J/kg.K in the chosen temperature range, while the DSC measurements varied from 4.196 to 4.240 J/kg.K with a standard deviation of 0.00929 J/kg.K, which agrees within 0.7 % from reported values in the same temperature range.

Measurements of CO₂ hydrate-ice mixture

Pure CO₂ hydrates are not easy to be generated inside a DSC due to constraints related to the required high pressure conditions and appropriate scanning characteristics. To reduce these complexities, CO₂ hydrate-ice mixture formation and dissociation was performed to obtain the dissociation enthalpy of pure CO₂ hydrate. Based on the described preliminary measurements, a DSC experimental procedure for the CO₂ hydrate-ice mixture was applied. Tap water mass was accurately weighed; a simple pressure panel was adapted to guarantee CO₂ gas pressure around 15 bar during the formation and dissociation process; the Micro DSCVII was cooled down to -15 °C with a scanning rate of 0.08 K/min to allow water crystallization and CO₂ hydrate formation; then the Micro DSCVII was heated up to 25 °C at a slow scanning rate of 0.15 K/min. After the ice melting, an endothermic peak linked with CO₂ hydrate dissociation was detected.

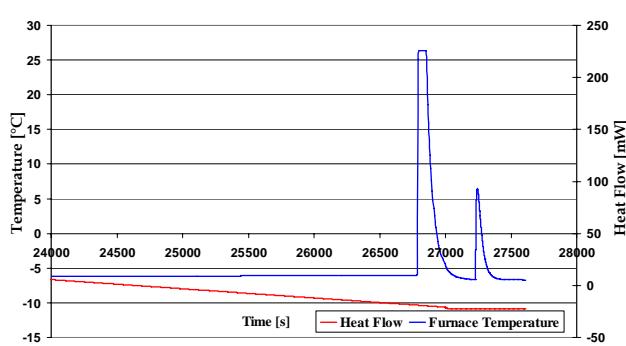


Figure 4a: The Formation of Ice and CO₂ Hydrate Mixture Micro DSCVII under 15 bar

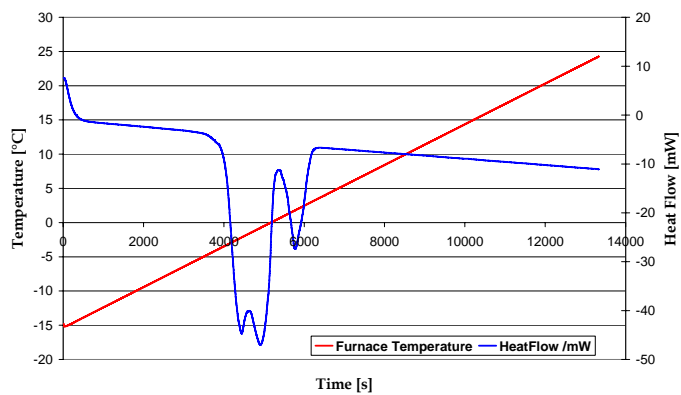


Figure 4b: The Dissociation of Ice and CO₂ Hydrate Mixture in the Vessel of the Micro DSCVII; the first peak refers to ice melting while the second peak refers to CO₂ hydrate dissociation

Figure 4a shows two exothermic peaks. The first large one corresponds to ice formation, while the second one relates to CO₂ hydrate formation. Ice formation occurs prior to hydrate formation. Since ice is easier to form in the DSC, a large portion of water formed ice, released a large amount of heat and only a small portion of water formed CO₂ hydrate. This explains the difference of sizes between the two observed peaks. Figure 4b shows two endothermic peaks. The first large one corresponds to ice dissociation process and the second one relates to CO₂ hydrate dissociation. Ice dissociation occurs prior to hydrate formation. Figure 4b also reveals that the mixture is mainly

composed of ice since the area (which equals energy) of the first peak is much larger than the one of the second peak. By integrating the area of the second peak, a CO_2 hydrate dissociation enthalpy value of 493 kJ/kg water is achieved, which is in very good agreement with the value measured by Marinhais *et al.* (2007), who reported a hydrate enthalpy equal to 500 kJ/kg of water.

4.3 Corrosion Rate of CO_2 Hydrate Slurry

During the experiment, several pH tests were carried out and values of saturated CO_2 solution as well as CO_2 hydrate slurry was found to be between 5.5 and 6. That means that the CO_2 solution and CO_2 hydrate slurry are both weak acidic substances. To study the corrosion effects of the CO_2 solution as well as the CO_2 hydrate slurry on low carbon steel, stainless steel and copper for the (future) air-conditioning industry, a complete cycle (creation and dissociation) of CO_2 hydrate slurry was conducted, which included: cooling down the saturated CO_2 solution from room temperature to a temperature around 1 to 2 °C and at a pressure range of 25 to 30 bar; injection of CO_2 gas to reach super saturation conditions; formation and cycling CO_2 hydrate slurry in the loop until the hydrate slurry reaches a temperature of approximately 6 °C; consuming of CO_2 hydrate slurry in the heat exchanger at a temperature above 6 °C until all CO_2 slurry dissociates (around 9 °C).

With the aid of probe tube fittings, the high pressure CS1018 low carbon steel, copper 110 and 304L stainless steel probes were vertically immersed in the CO_2 hydrate slurry transportation pipes. The experiments were conducted at a temperature ranging from 1 to 18 °C and pressure ranging from 25 to 30 bar. High pressure probes were subjected to a complete cycle of CO_2 hydrates slurry formation and dissociation and transferred signals to CMAS analyzer S-50. For stabilisation purposes, CMAS was turned on for more than two hours before monitoring.

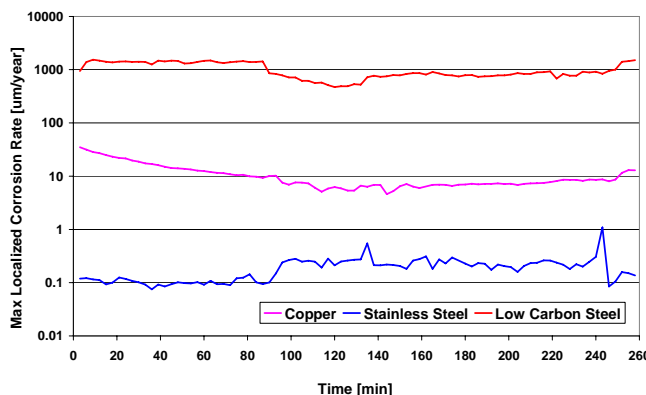


Figure 5a: Maximum Localised Corrosion Rates of Different Material Probes during a Short-Term Testing in the CO_2 Hydrate Slurry Loop

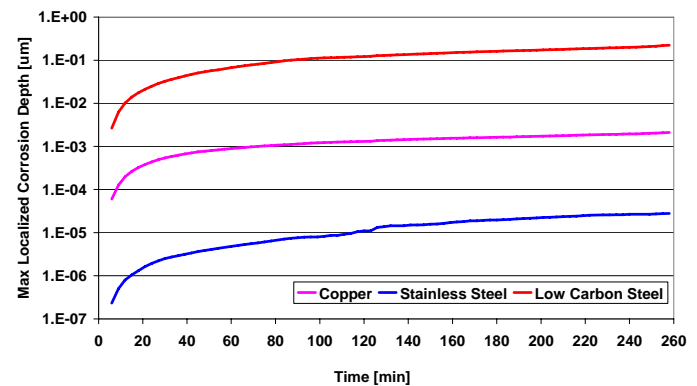


Figure 5b: Maximum Localised Corrosion Penetration Depth Measured from the Probes

Figure 5 shows the maximal localised penetration rates for type 304L stainless steels, type copper 110 and type 1018 low carbon steel. The stabilised maximum localised corrosion rates for the three metals varied by nearly 5 orders of magnitude. Short-term experimental results show that type 304L stainless steel and copper 110 displayed very good resistance to the corrosion caused by CO_2 hydrate slurry, while type 1018 low carbon steel had very poor resistance to the corrosion. The maximum localised corrosion penetration depths are shown in Figure 5b. Metal damage on the 304L stainless steel was smallest while on the 1018 low carbon steel it was largest.

5. CONCLUSION AND OUTLOOK

By testing with water, all measurement devices and techniques employed in this work were shown to be reliable and repeatable. The density and viscosity of the CO₂ solution were found to decrease with increasing temperature and increase with increasing pressure. High pressures and low temperatures conditions were found to favour the dissolution of CO₂ gas into water resulting in higher viscosity of the solution. In other words, the viscosity of the CO₂ solution depends on the CO₂ solubility. Formation of the CO₂ hydrate slurry from saturated CO₂ solution revealed that the CO₂ hydrate solid contributes only slightly to the viscosity increase resulting in excellent pumpability characteristics regarding power consumption even for a very high density. Experimental results also imply that the interactions between CO₂ molecules and water molecules are dependent on the pressure and temperature conditions and, therefore, influence the viscosity. A large number of hydrogen-bonded CO₂ hydrate precursor, which may form in the supersaturated solution before nucleation of hydrates also cause the increase of viscosity. The density of CO₂ hydrate slurry depends on the solid concentration of pure hydrates. At a suitable hydrate formation temperature range, the density of CO₂ hydrate slurry increases with increasing pressure. The CO₂ hydrates dissociation enthalpy was measured by means of a DSC and equals 493 kJ/kg of water, which is in good agreement with the available literature data. On-line measurement of corrosion rate have demonstrated that although CO₂ hydrate slurry is a kind of weak acidified substance, it still has negative effects on three test metals when considering a long term application. Experimental results in this paper provide important reference data in selecting different materials for the applications of CO₂ hydrate slurry in air conditioning industry, cold storage and other applications. In the near future, on-line measurement of thermal conductivity will be carried out; and an equation of viscosity of CO₂ hydrate slurry as a function of the solubility will be established.

REFERENCES

Anderson, V., Flow properties of natural gas hydrate slurries an experimental study, Ph.D thesis, December 1999.

Anderson, V. and Gudmundsson, J.S., (2000). Flow Properties of Hydrate-in-Water Slurries, *Annals of the New York Academy of Sciences* 912:322-329.

Bozzo, A.T., Chen, H.-S., Kass, J.R. and Barduhn, A.J., (1975), Desalination, 16, 303–320.

Duan, Z., Hu, J., Li, D. and Mao, S. (2008). "Density of the CO₂-H₂O and CO₂-H₂O-NaCl Sytems Up to 647 K and 100 MPa." Energy and Fuels

Fenghour, A., Wakeham, W.A. and Vesovic, V. (1998). "The Viscosity of Carbon Dioxide". J. Phys. Chem. Ref. Data 27(1): 31-44.

Garcia, J. E., (2001). Density of Aqueous Solutions of CO₂. California, Lawrence Berkeley National Laboratory, University of California.

Grunberg L. and Nissan A. H., (1949). *Nature* (London), **164**, 799-800.

Marinhas, S., Delahaye, A., Fournaison, L., Dalmazzone, D., Furst, W. and Petitet, J-P., (2006). "Modelling of the Available Latent Heat of a CO₂ Hydrate Slurry in an Experimental loop Applied to Secondary Refrigeration." *Chem. Eng. and Processing* 45: 184-192.

Oyama, H., Ebinuma, T., Shimada, W., Takeya, S., Nagao, J., Uchida, T. and Narita, H. (2003). "An Experimental Study of Gas-Hydrate Formation by Measuring Viscosity and Infrared Spectra." *Can. J. Phys.* 81: 485-492.

Sloan, E.D., (2004). "Introductory overview: Hydrate knowledge development", *Amer. Mineralogist*, **89**, 1155-1161

Span, R. and Wagner, W. (1996). "A New Equation of State for Carbon Dioxide Covering the Fluid Region from Triple-Point Temperature to 1100 K at Pressures Up to 800 MPa." J. Phys. Chem. Ref. Data 25: 1509-94.

Teng, H., Yamasaki, A. and Shindo, Y. (1996). "Stability of the Hydrate Layer Formed on the Surface of a CO₂ Droplet in High Pressure, Low Temperature Water." *Chem. Eng. Sci.* 51(22): 4979-4986.

Uchida, T., Ohmura, R., Nagao, J., Takeya, S., Ebinuma, T. and Narita, H. (2003). "Viscosity of Aqueous CO₂ Solutions Measured by Dynamic Light Scattering." *J. Chem. Eng. Data* 48: 1225-1229.

Wagner, W. and Pruess, A. (2002). "The IAPWS Formulation 1995 for the Thermodynamic Properties of Ordinary Water Substance for General and Scientific Use." J. Phys. Chem. Ref. Data 31(2): 387-535.

Watson, J. T. R., Basu, R.S. and Sengers, J.V. (1980). "An Improved Representative Equation for the Dynamic Viscosity of Water Substance." J. Phys. Chem. Ref. Data 9(4): 1255-1290.

ACKNOWLEDGEMENT

We acknowledge the financial support of the Office Fédéral de l'Energie (OFEN) Switzerland, Commission pour la promotion de la Technologie et l'Innovation (CTI), Switzerland and the "Haute Ecole Spécialisée de Suisse Occidentale" (HES-SO).